

Synthesis, crystal structure, Hirshfeld surfaces analysis, interaction with DNA and comparison of different bases in Hirshfeld Atom Refinement (HAR) of new polymorph of chlorido(η^6 -p-cymene)(diclofenac)ruthenium(II) organometallic compound.

Martin Schoeller ^{1*}, Milan Piroš ¹, Karol Lušpai ³, Jana Braniša ² and Ján Moncol ^{1,2*}

¹ Department of Inorganic Chemistry, Slovak University of Technology, Radlinského 9, 812 37 Bratislava, Slovakia

² Department of Chemistry, Faculty of Natural Sciences, Constatine the Philosopher University in Nitra, 949 74 Nitra, Slovakia

³ Department of Physical Chemistry, Slovak University of Technology, Radlinského 9, 812 37 Bratislava, Slovakia

Supplementary material

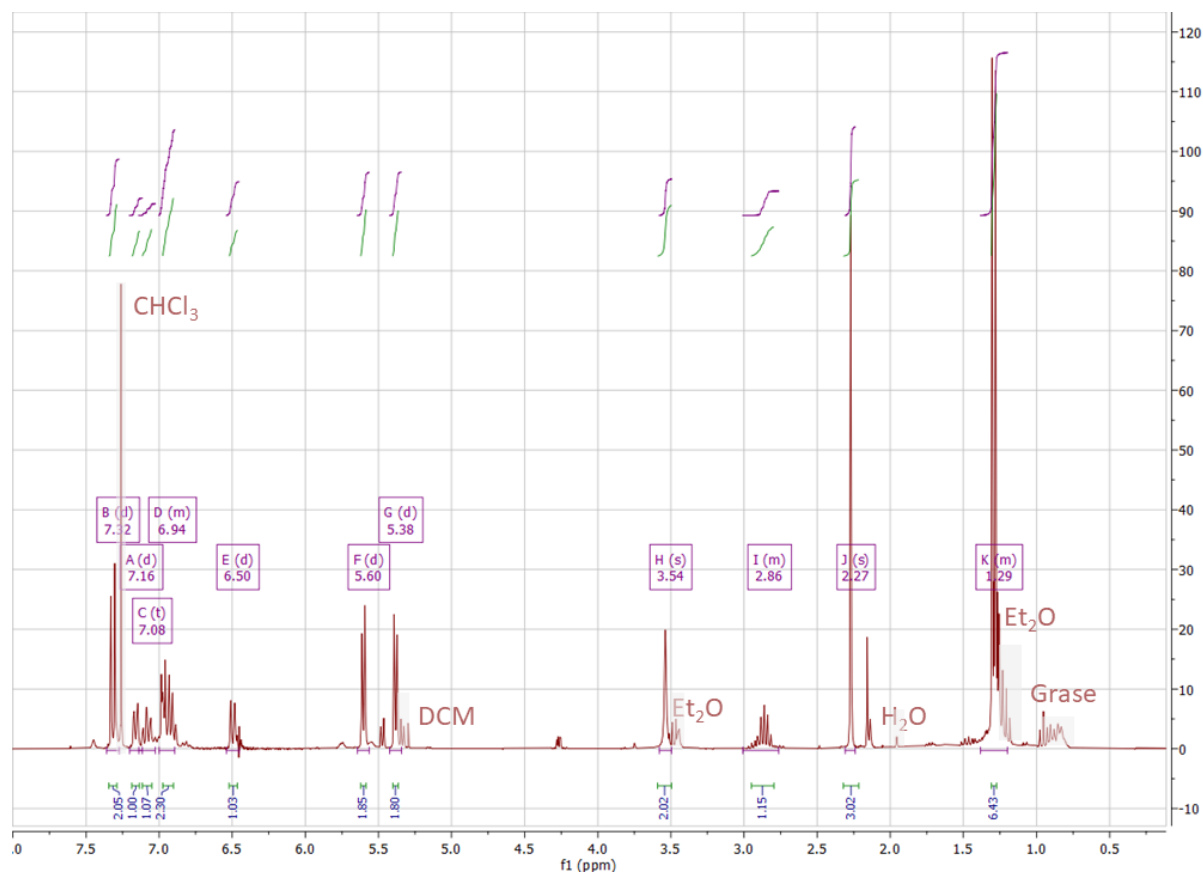


Figure S1 The ¹H NMR spectrum of prepared complex

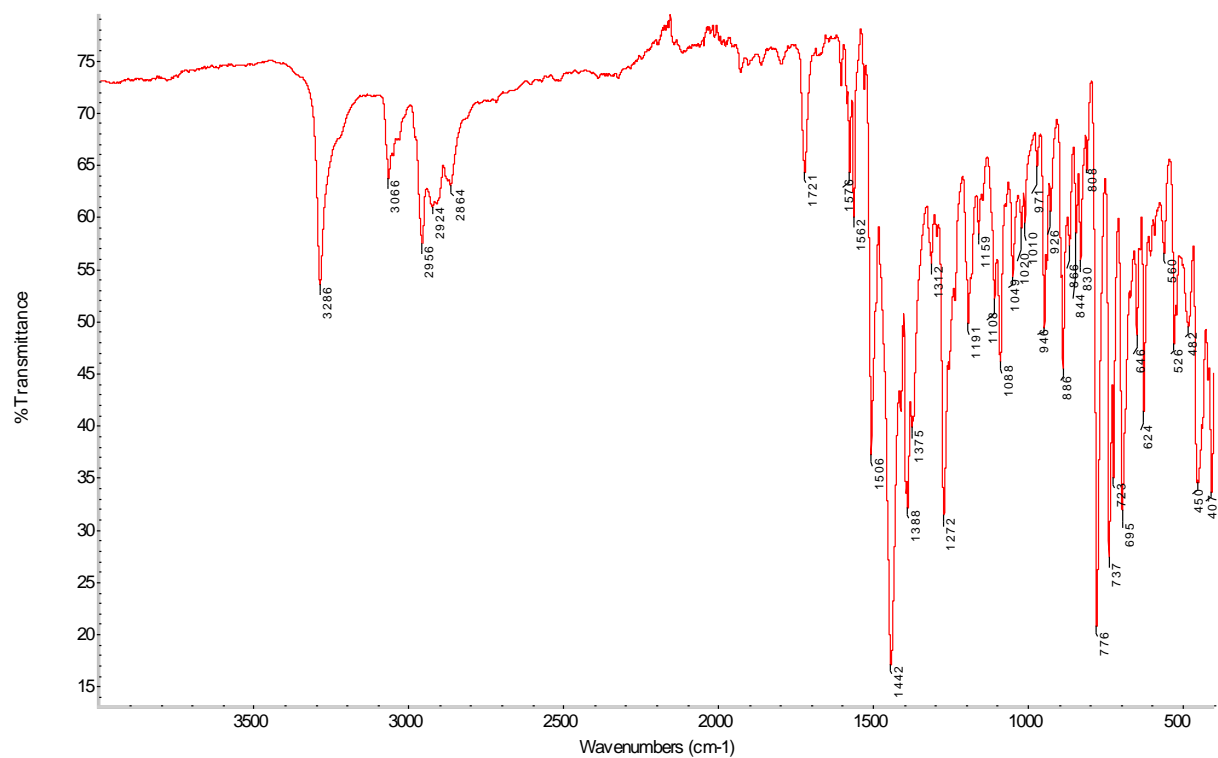


Figure S2 The FTIR spectrum of prepared complex

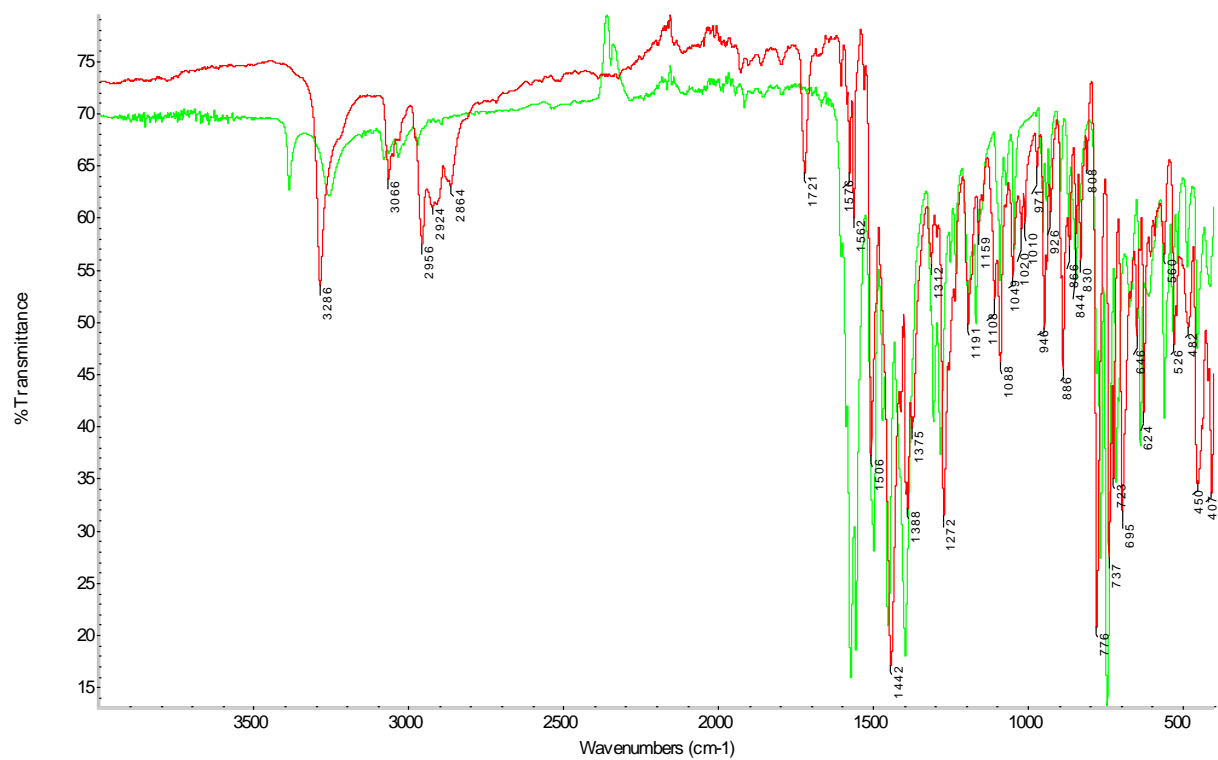


Figure S3 Comparison of FTIR spectra of prepared complex and diclofenac sodium salt



Figure S4 Comparison of FTIR spectra of prepared complex and dimeric precursor

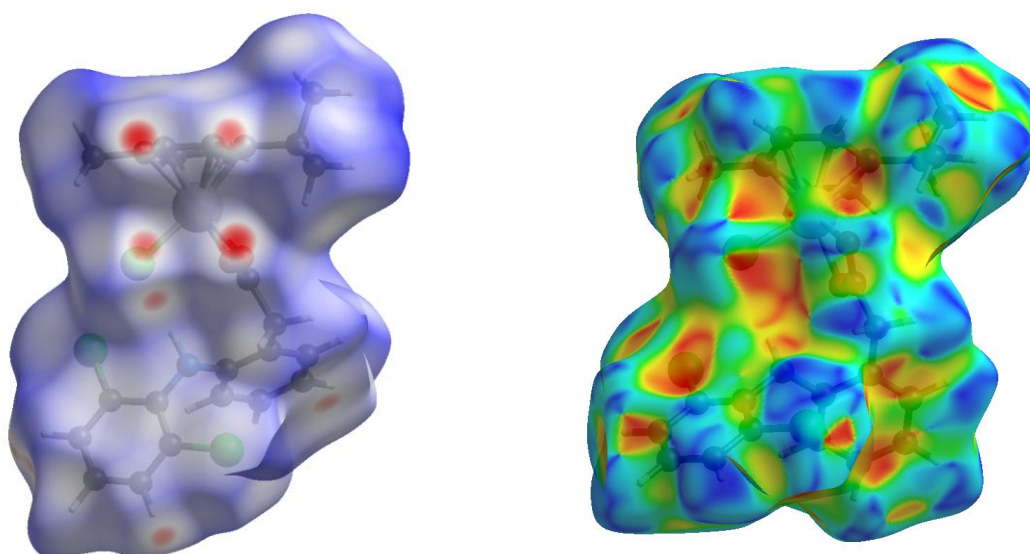


Figure S5 Hirshfeld surface for HAR1 model of complex mapped over d_{norm} (left) and shape index (right)

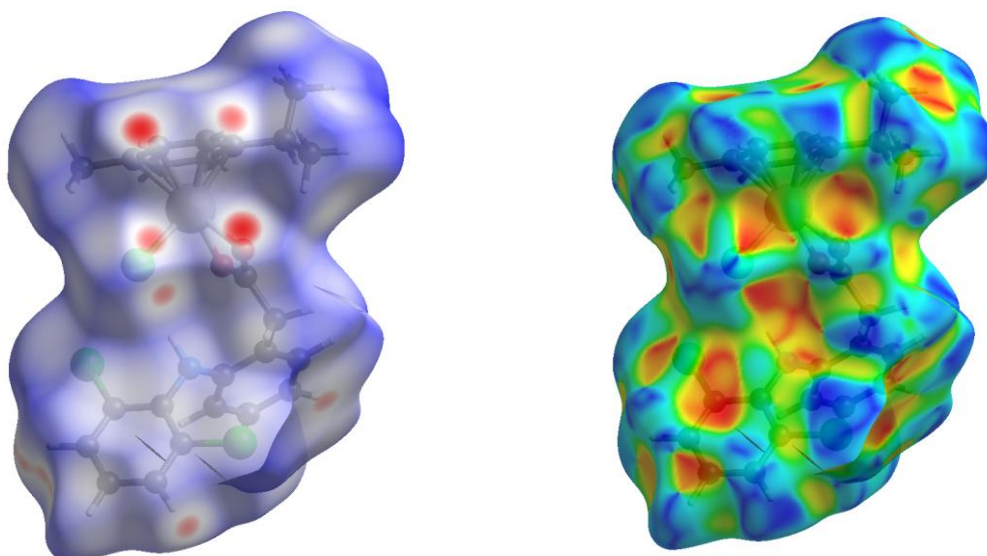


Figure S6 Hirshfeld surface for HAR2 model of complex mapped over d_{norm} (left) and shape index (right)

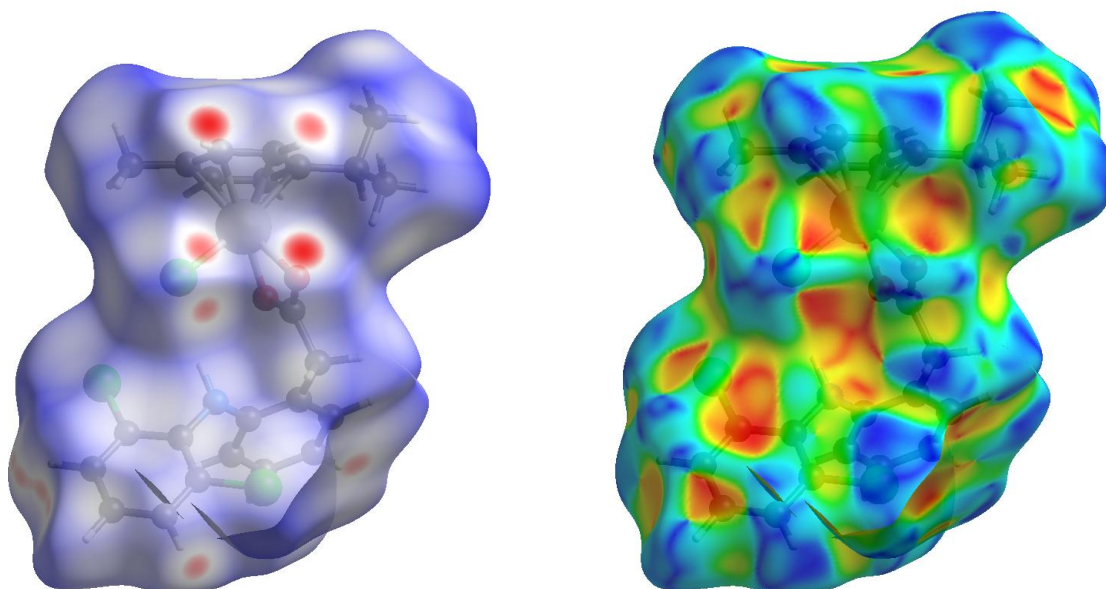


Figure S7 Hirshfeld surface for HAR3 model of complex mapped over d_{norm} (left) and shape index (right)

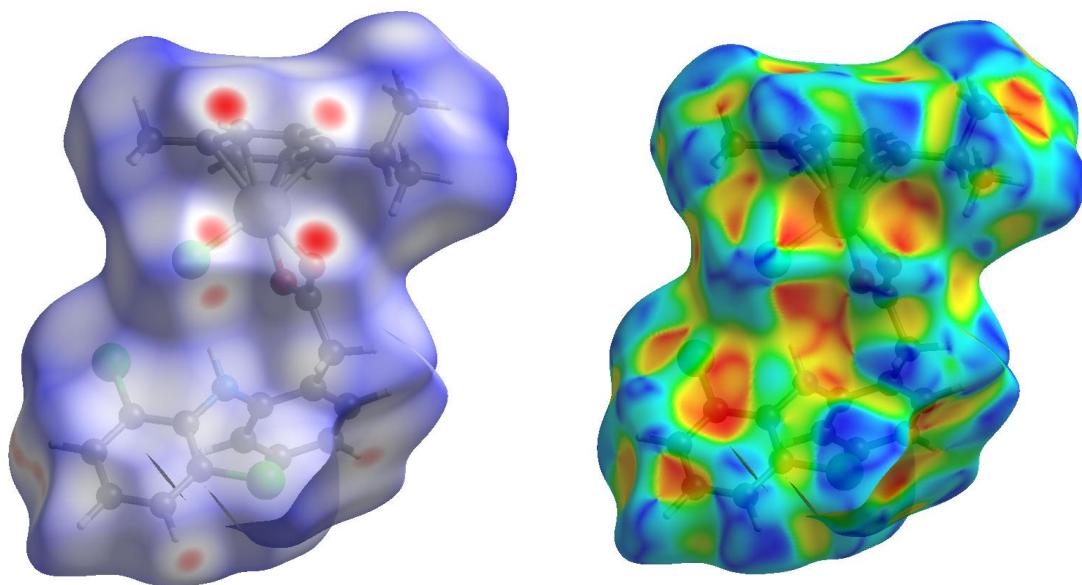


Figure S8 Hirshfeld surface for HAR4 model of complex mapped over d_{norm} (left) and shape index (right)

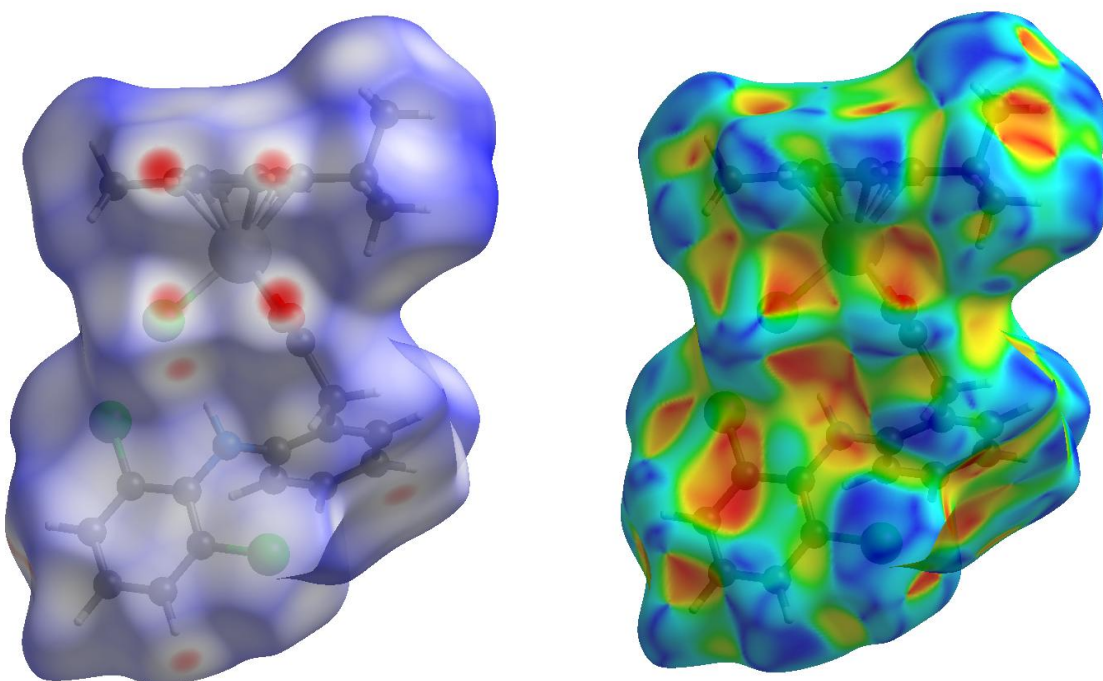


Figure S9 Hirshfeld surface for HAR5 model of complex mapped over d_{norm} (left) and shape index (right)

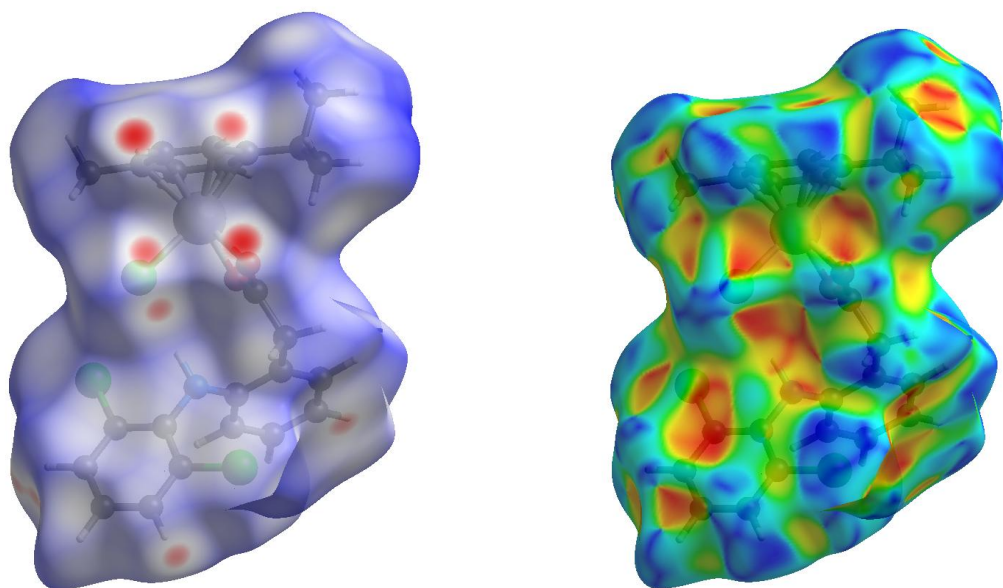


Figure S10 Hirshfeld surface for HAR6 model of complex mapped over d_{norm} (left) and shape index (right)

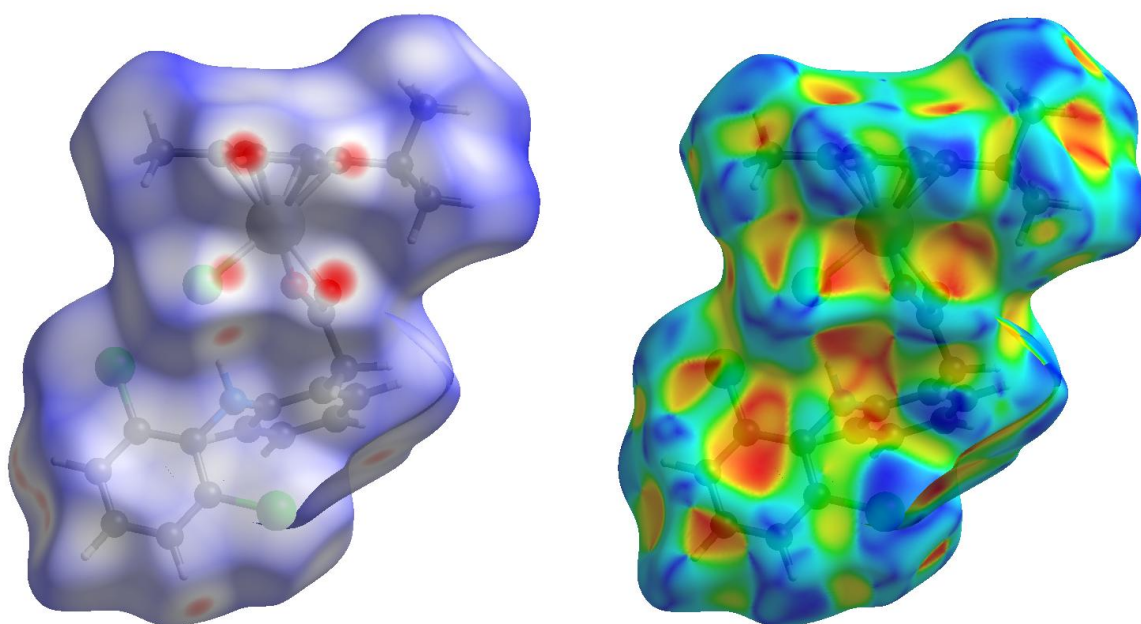


Figure S11 Hirshfeld surface for HAR7 model of complex mapped over d_{norm} (left) and shape index (right)

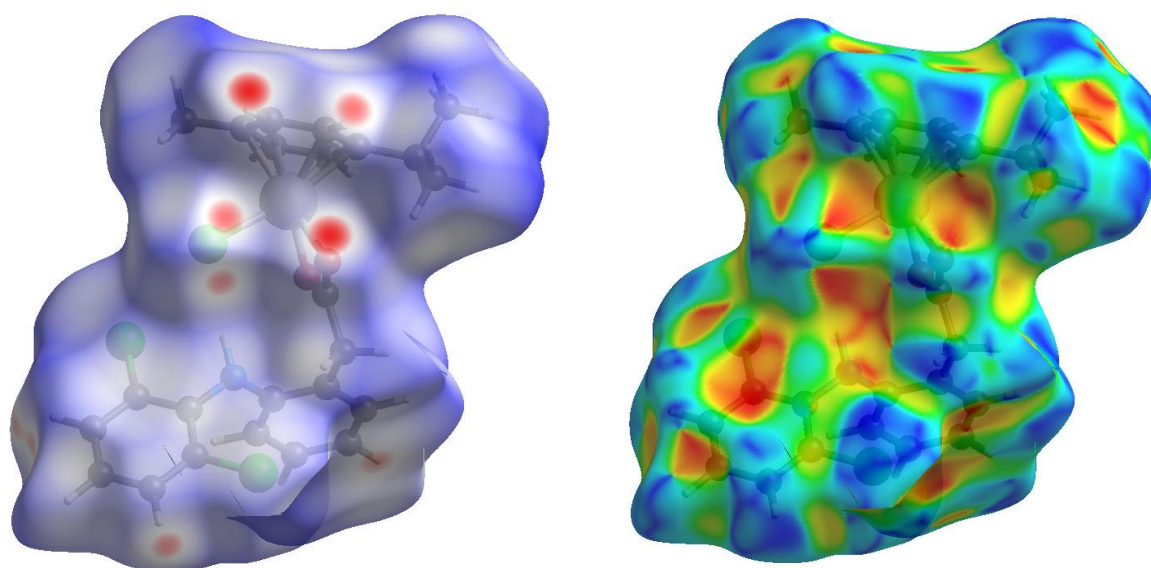


Figure S12 Hirshfeld surface for HAR8 model of complex mapped over d_{norm} (left) and shape index (right)

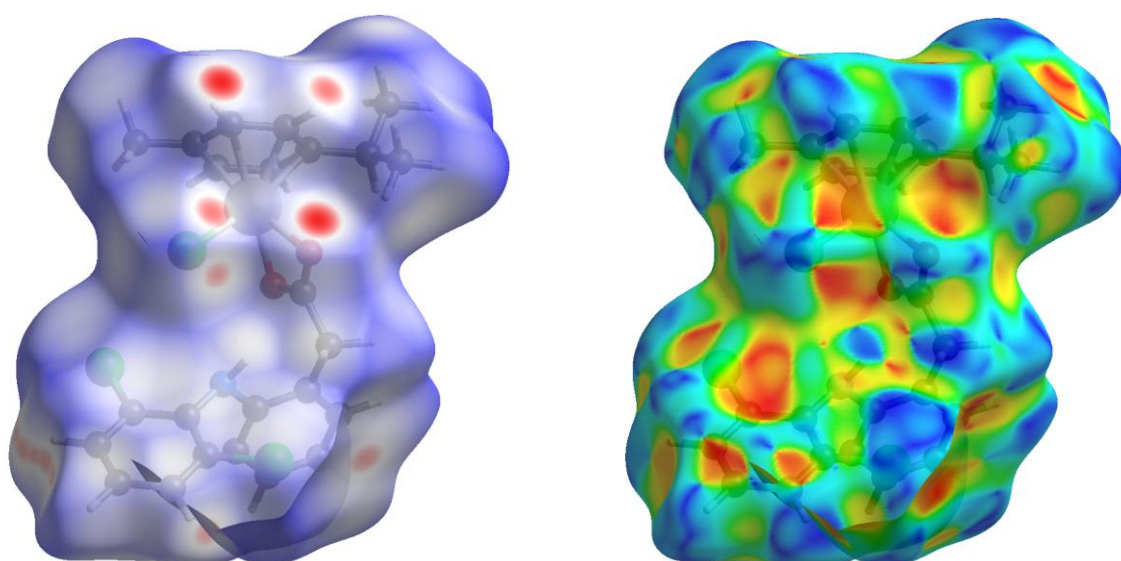


Figure S13 Hirshfeld surface for prepared complex with non-HAR (IAM) model of complex mapped over d_{norm} (left) and shape index (right)

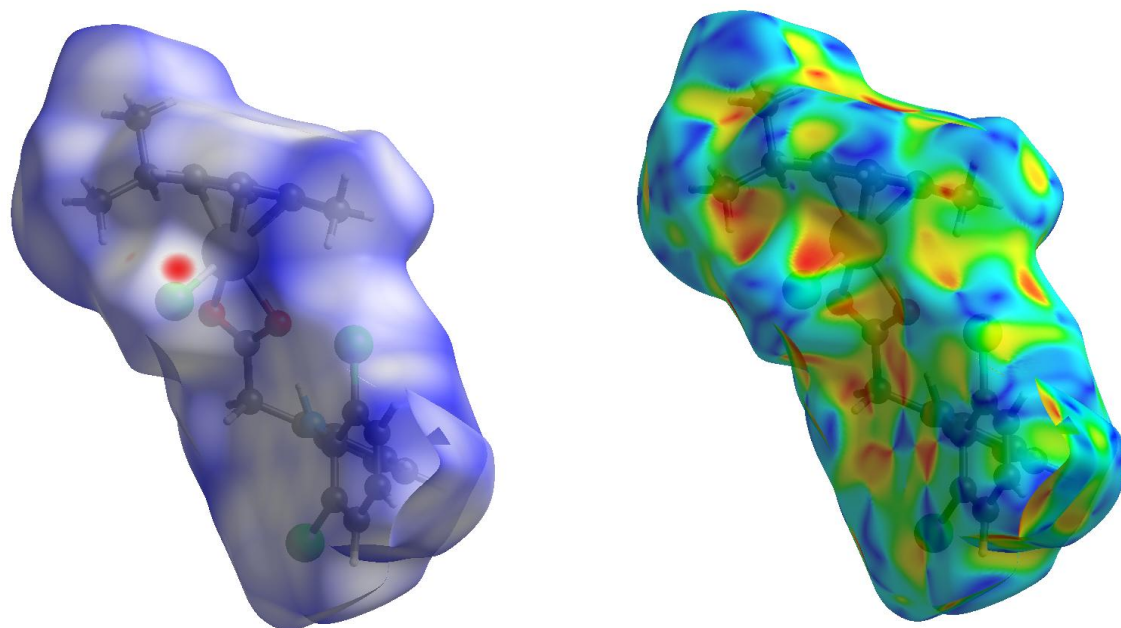


Figure S14 Hirshfeld surface for orthorhombic polymorph of complex mapped over d_{norm} (left) and shape index (right) [35]

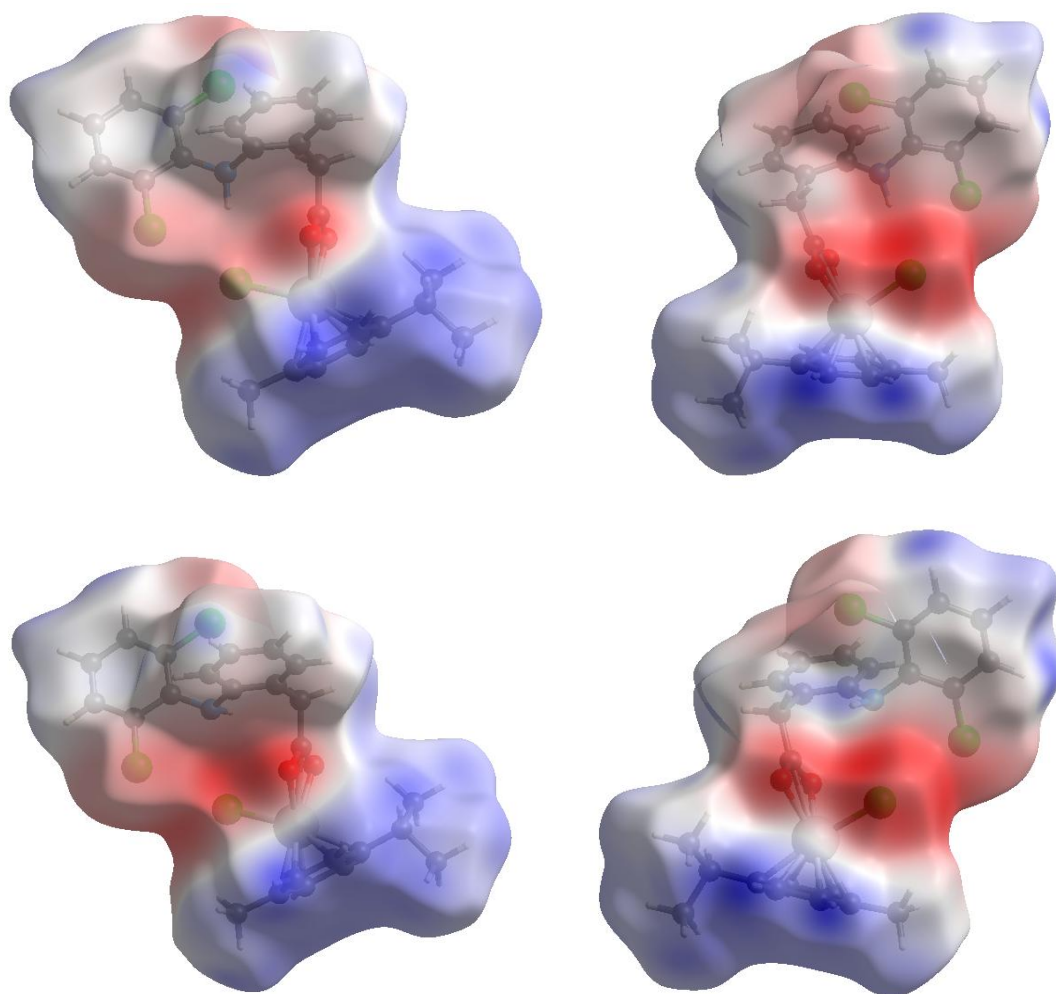


Figure S15 Hirshfeld surface mapped over the electrostatic potential of 1 (top) and orthorhombic polymorph (bottom), with positive and negative potential indicated in blue and red, respectively.

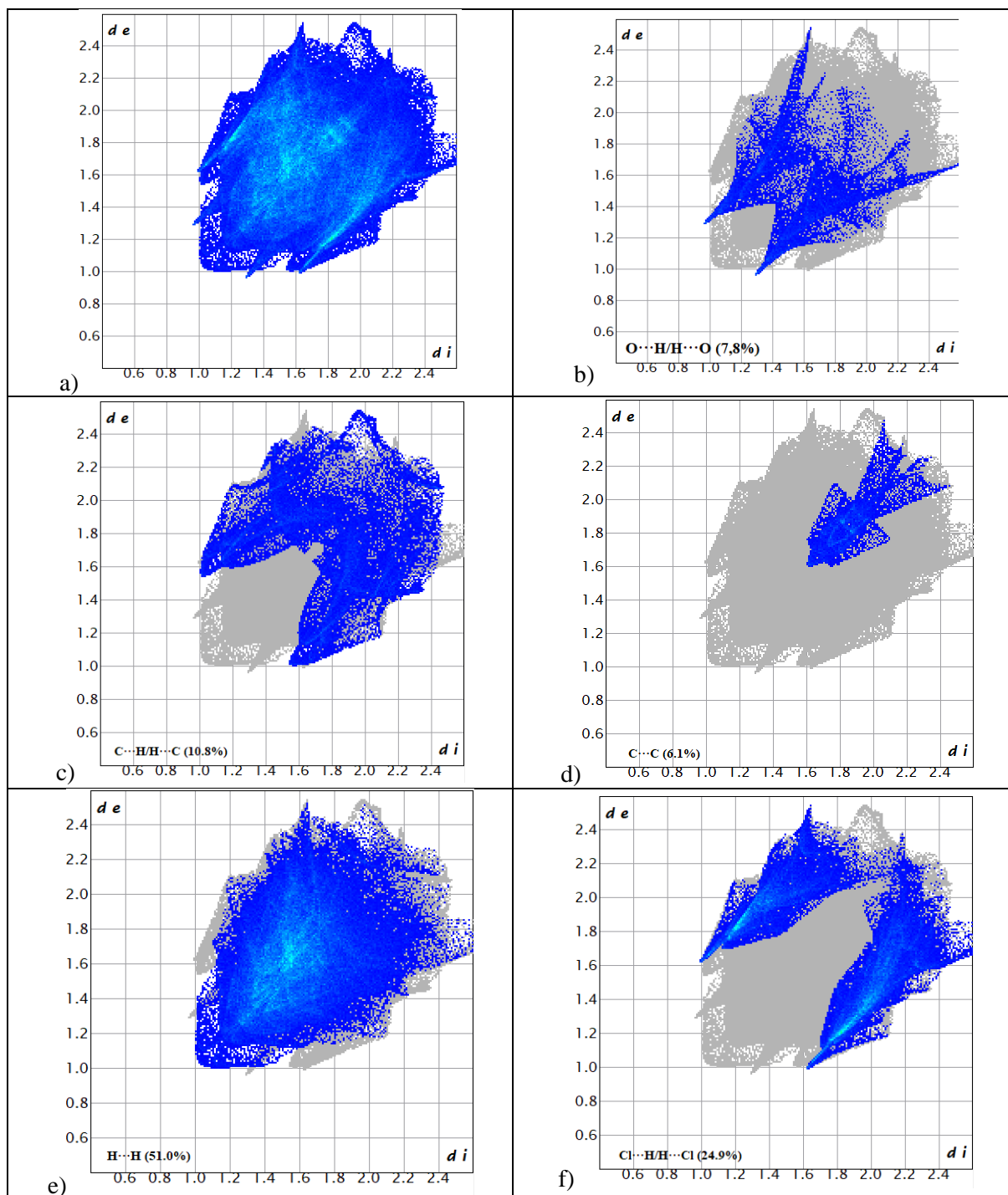


Figure S16 The full two-dimensional fingerprint plots of prepared complex (IAM model), showing a) all interactions, b) $O \cdots H/H \cdots O$, c) $C \cdots H/H \cdots C$, d) $C \cdots C$, e) $H \cdots H$, and f) $Cl \cdots H/H \cdots Cl$ close contacts.

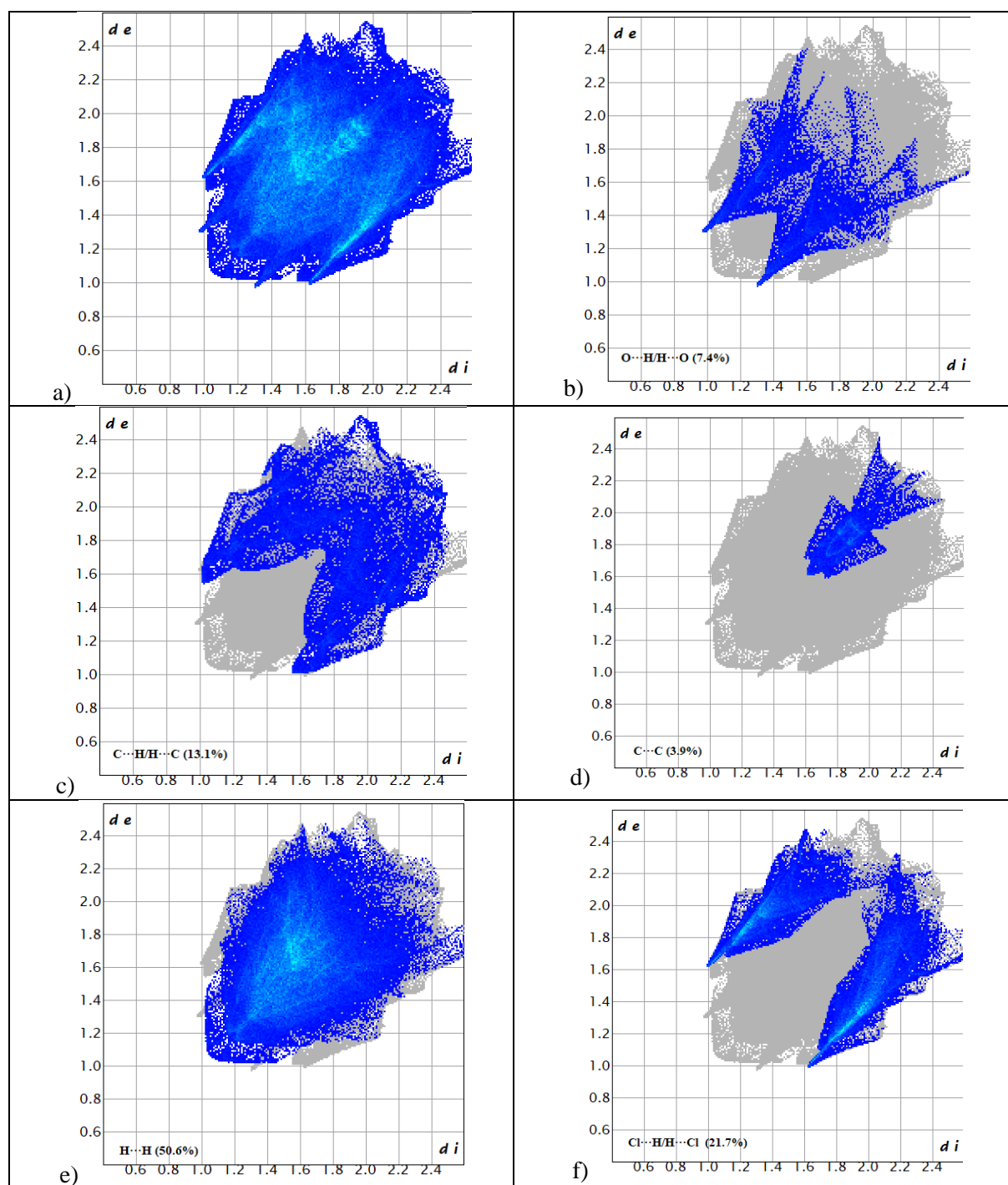


Figure S17 The full two-dimensional fingerprint plots of HAR1 model of prepared complex, showing a) all interactions, b) $O \cdots H/H \cdots O$, c) $C \cdots H/H \cdots C$, d) $C \cdots C$, e) $H \cdots H$, and f) $Cl \cdots H/H \cdots Cl$ close contacts.

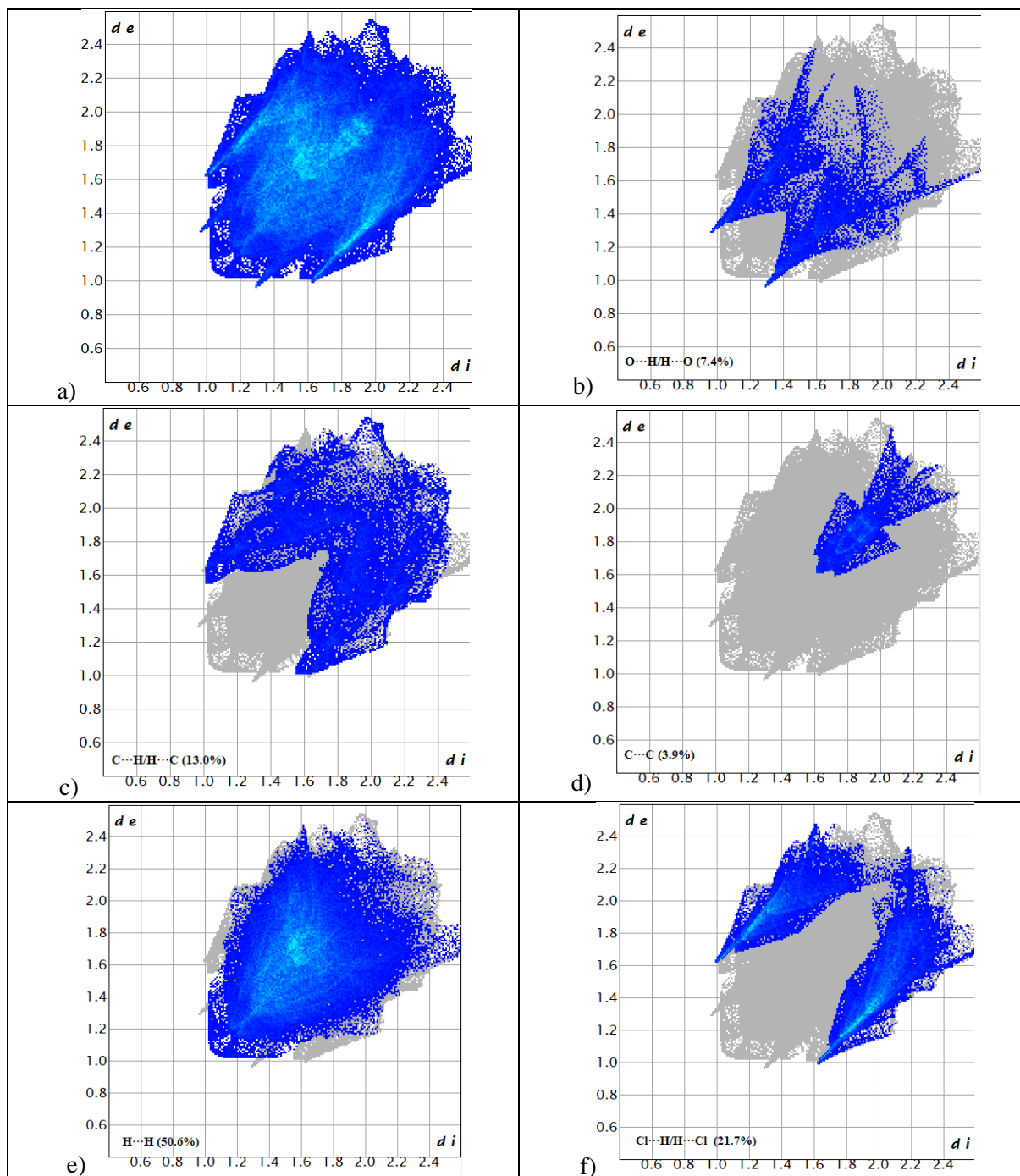


Figure S18 The full two-dimensional fingerprint plots of HAR2 model of prepared complex, showing a) all interactions, b) $\text{O}\cdots\text{H}/\text{H}\cdots\text{O}$, c) $\text{C}\cdots\text{H}/\text{H}\cdots\text{C}$, d) $\text{C}\cdots\text{C}$, e) $\text{H}\cdots\text{H}$, and f) $\text{Cl}\cdots\text{H}/\text{H}\cdots\text{Cl}$ close contacts.

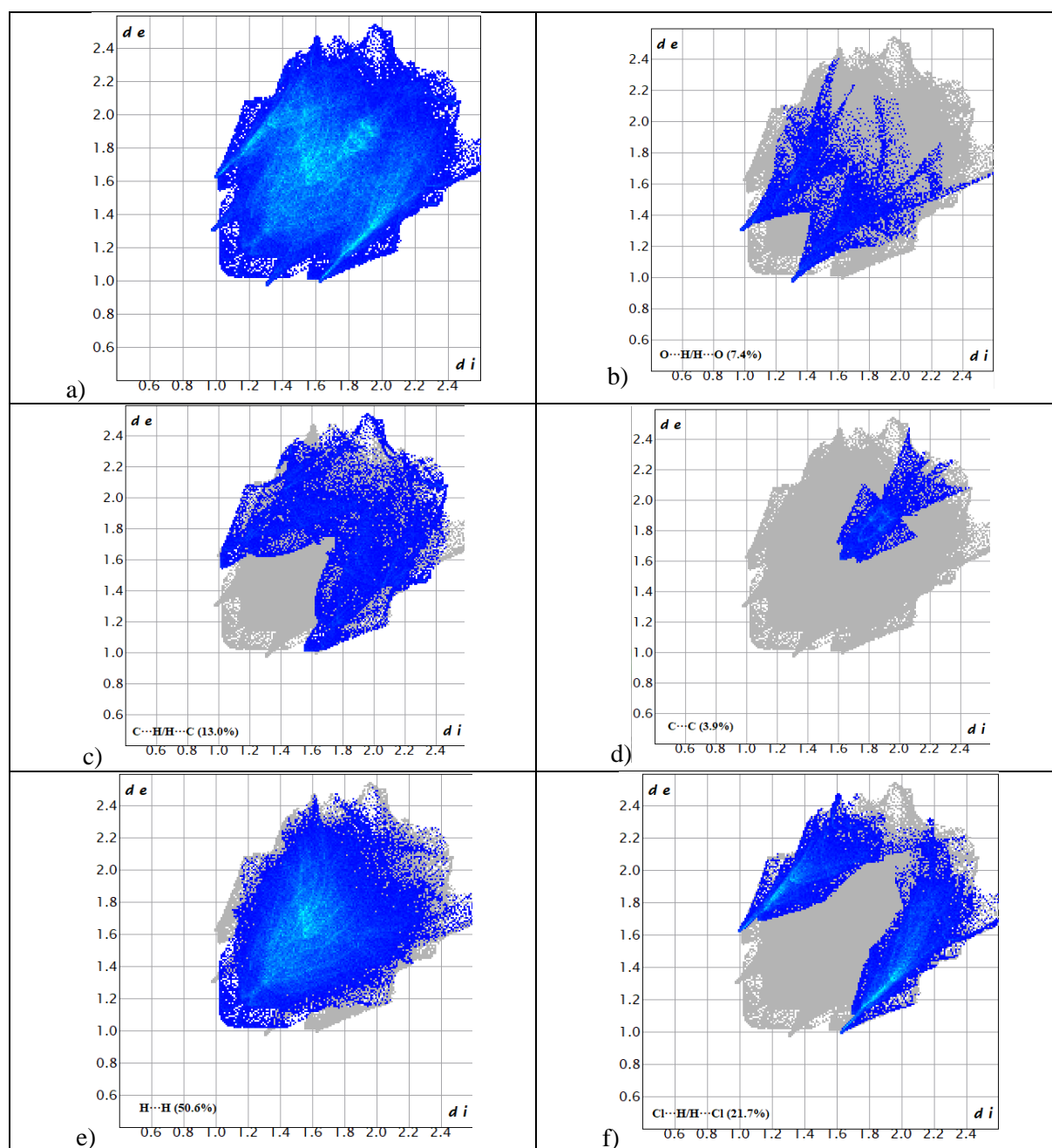


Figure S19 The full two-dimensional fingerprint plots of HAR3 model of prepared complex, showing a) all interactions, b) $O \cdots H/H \cdots O$, c) $C \cdots H/H \cdots C$, d) $C \cdots C$, e) $H \cdots H$, and f) $Cl \cdots H/H \cdots Cl$ close contacts.

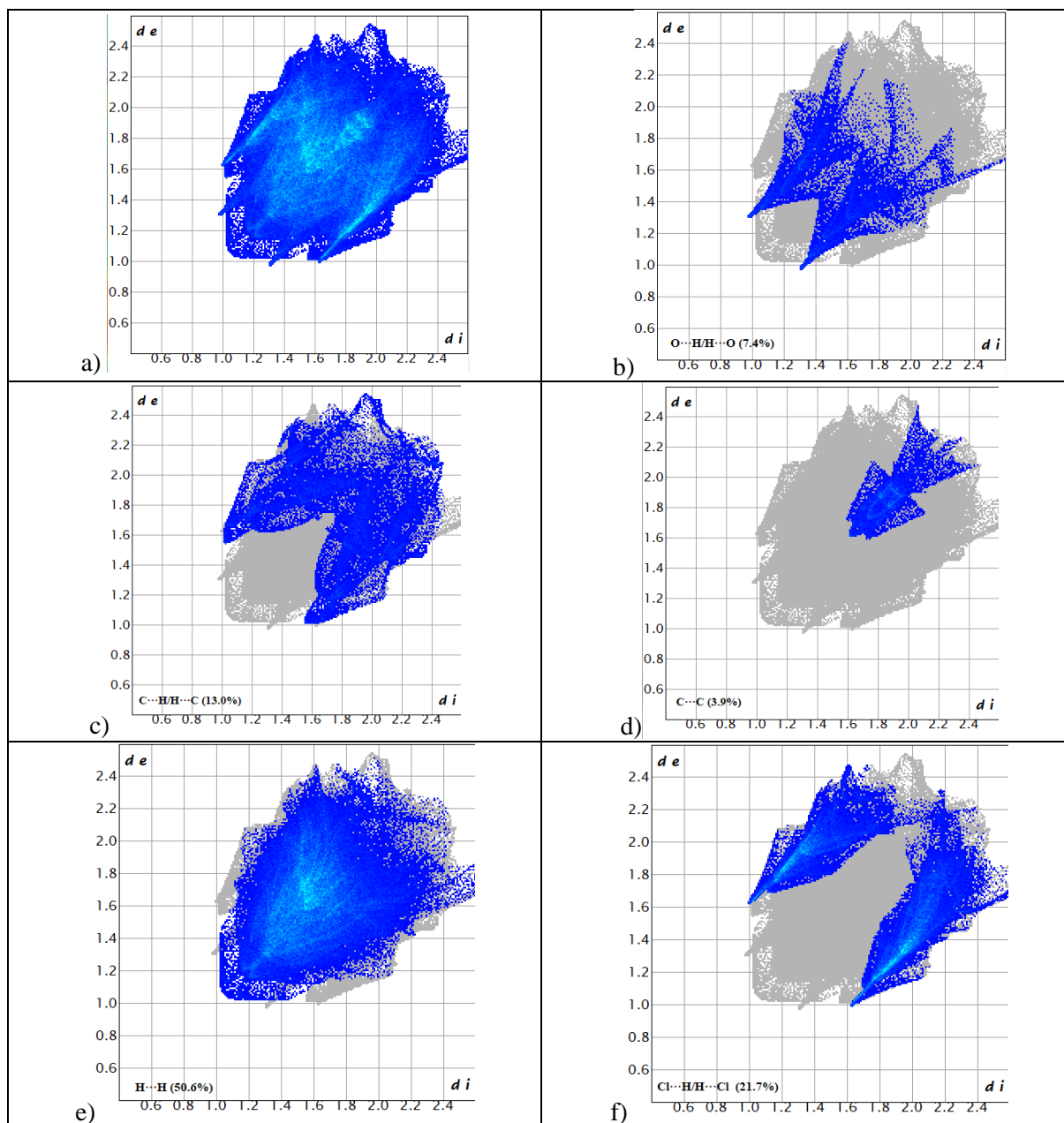


Figure S20 The full two-dimensional fingerprint plots of HAR4 model of prepared complex, showing a) all interactions, b) $O \cdots H/H \cdots O$, c) $C \cdots H/H \cdots C$, d) $C \cdots C$, e) $H \cdots H$, and f) $Cl \cdots H/H \cdots Cl$ close contacts.

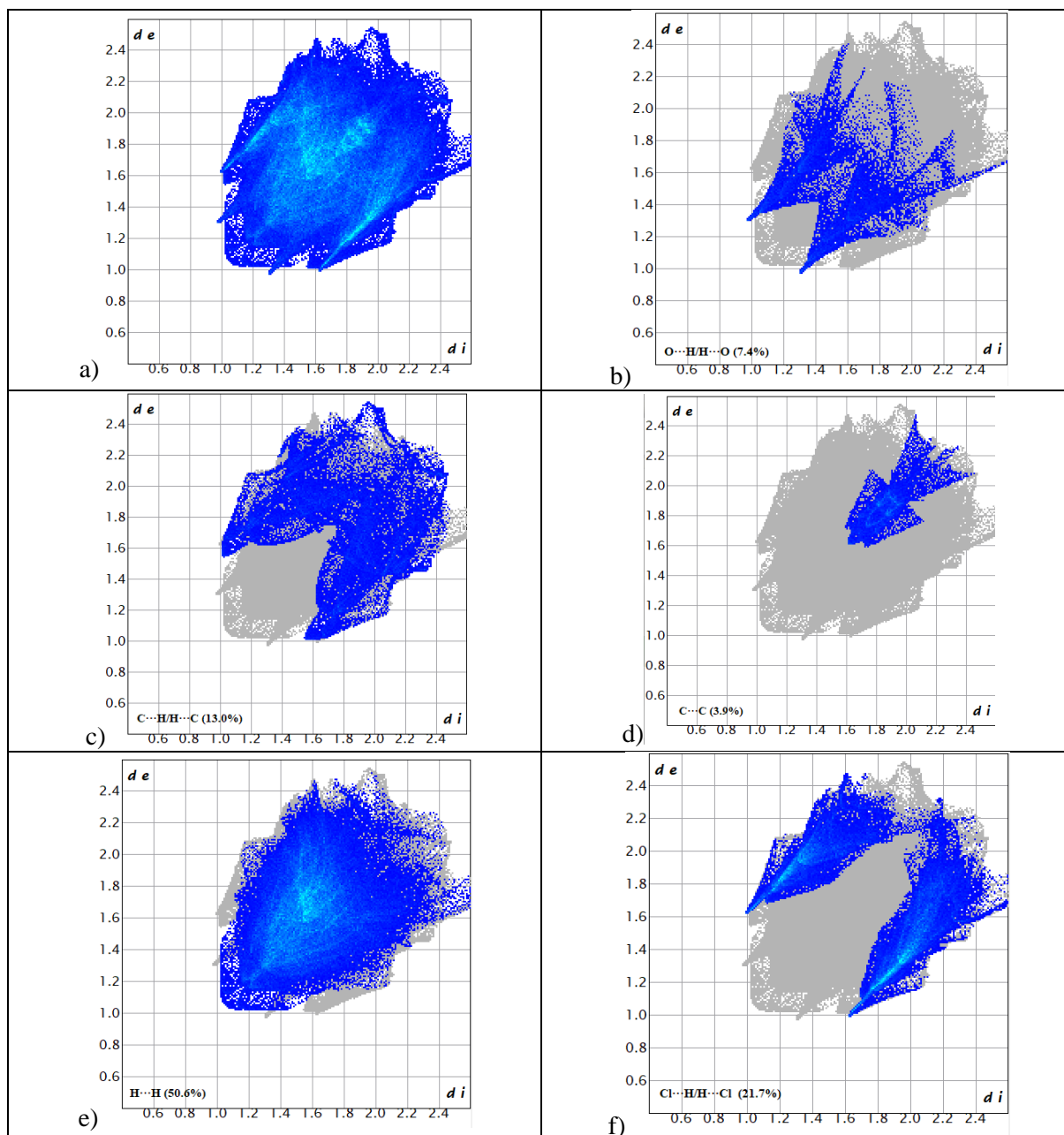


Figure S21 The full two-dimensional fingerprint plots of HAR5 model of prepared complex, showing a) all interactions, b) $O \cdots H/H \cdots O$, c) $C \cdots H/H \cdots C$, d) $C \cdots C$, e) $H \cdots H$, and f) $Cl \cdots H/H \cdots Cl$ close contacts.

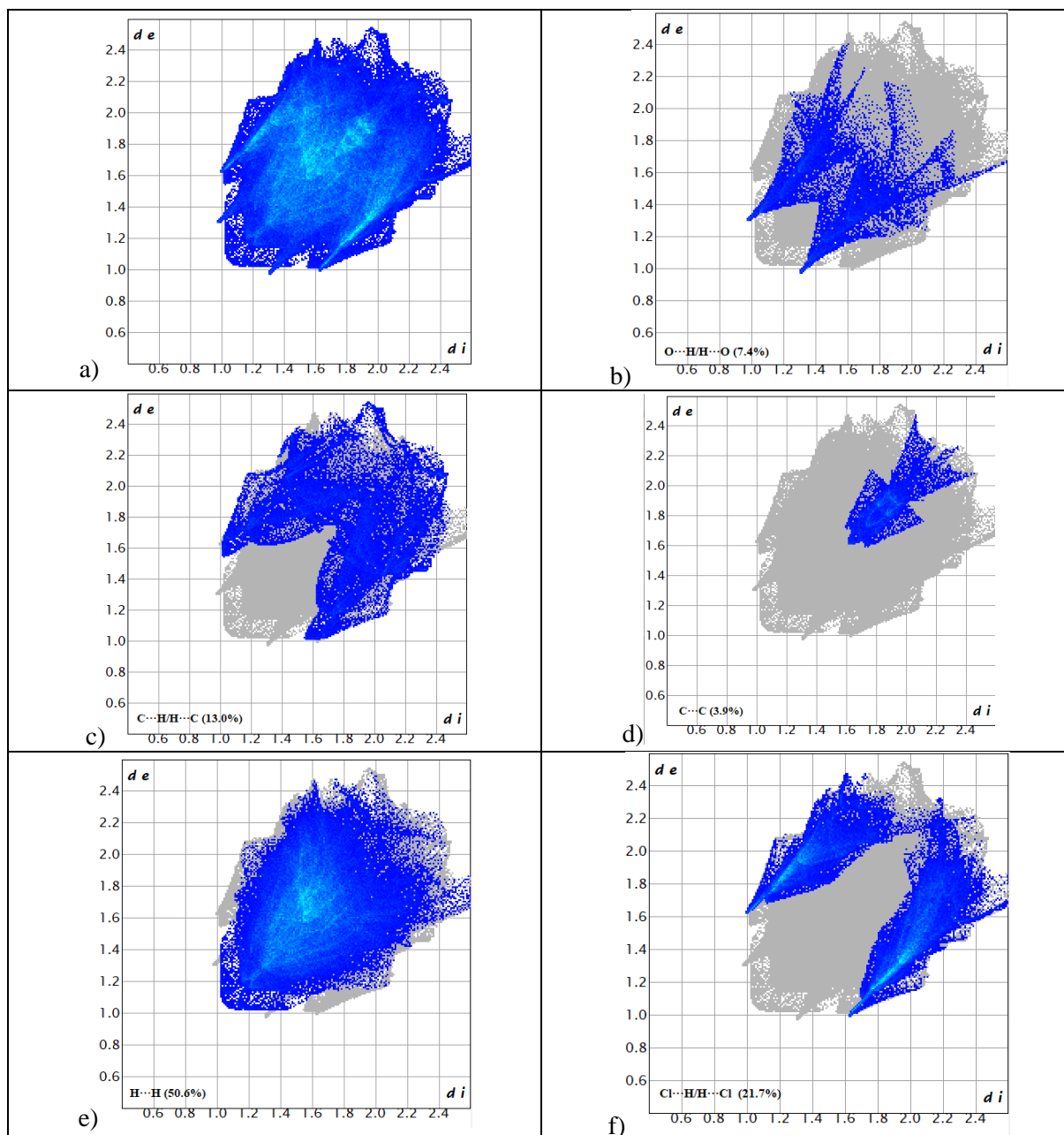


Figure S22 The full two-dimensional fingerprint plots of HAR6 model of prepared complex, showing a) all interactions, b) $O \cdots H/H \cdots O$, c) $C \cdots H/H \cdots C$, d) $C \cdots C$, e) $H \cdots H$, and f) $Cl \cdots H/H \cdots Cl$ close contacts.

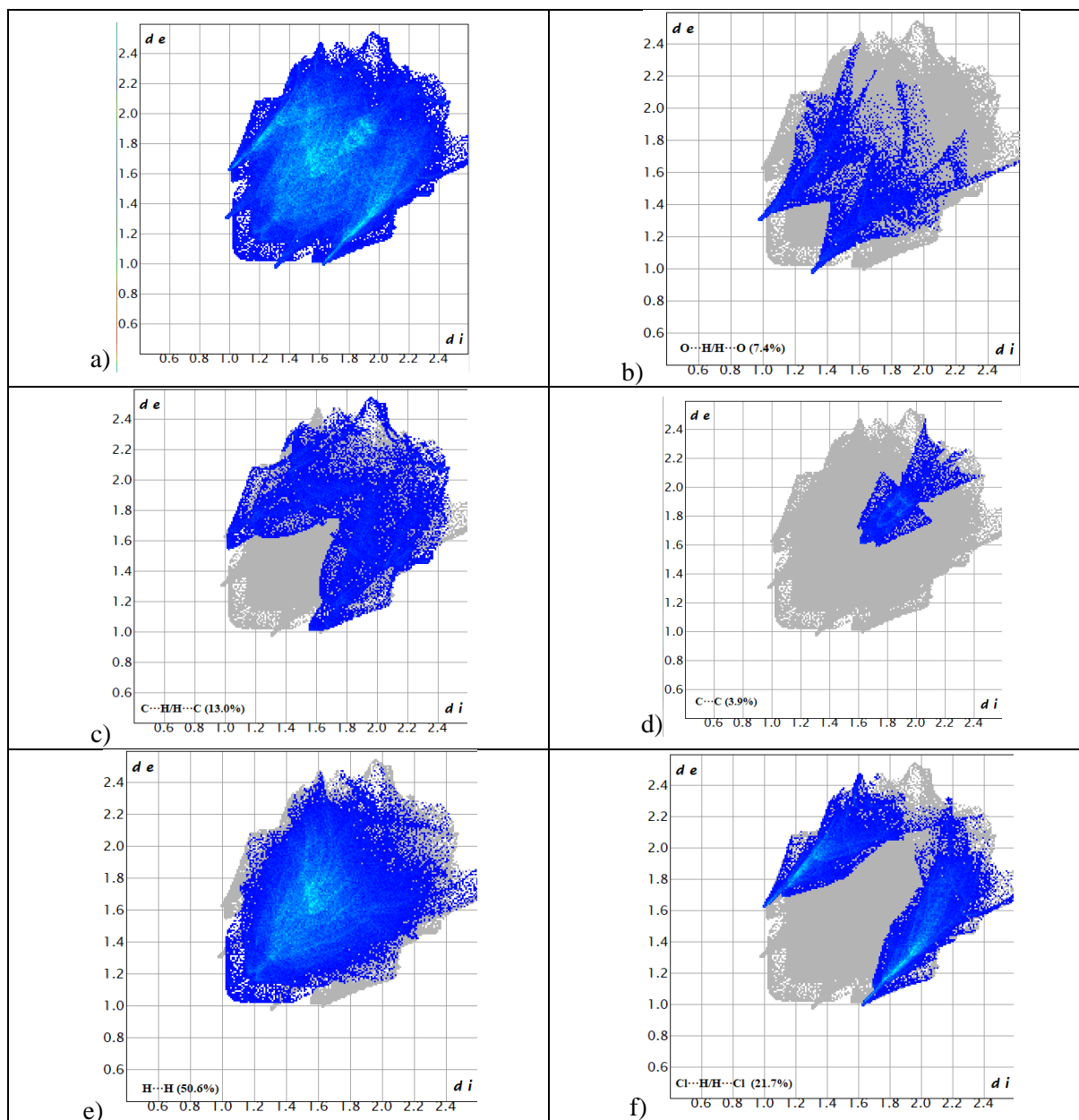


Figure S23 The full two-dimensional fingerprint plots of HAR7 model of prepared complex, showing a) all interactions, b) $O \cdots H/H \cdots O$, c) $C \cdots H/H \cdots C$, d) $C \cdots C$, e) $H \cdots H$, and f) $Cl \cdots H/H \cdots Cl$ close contacts.

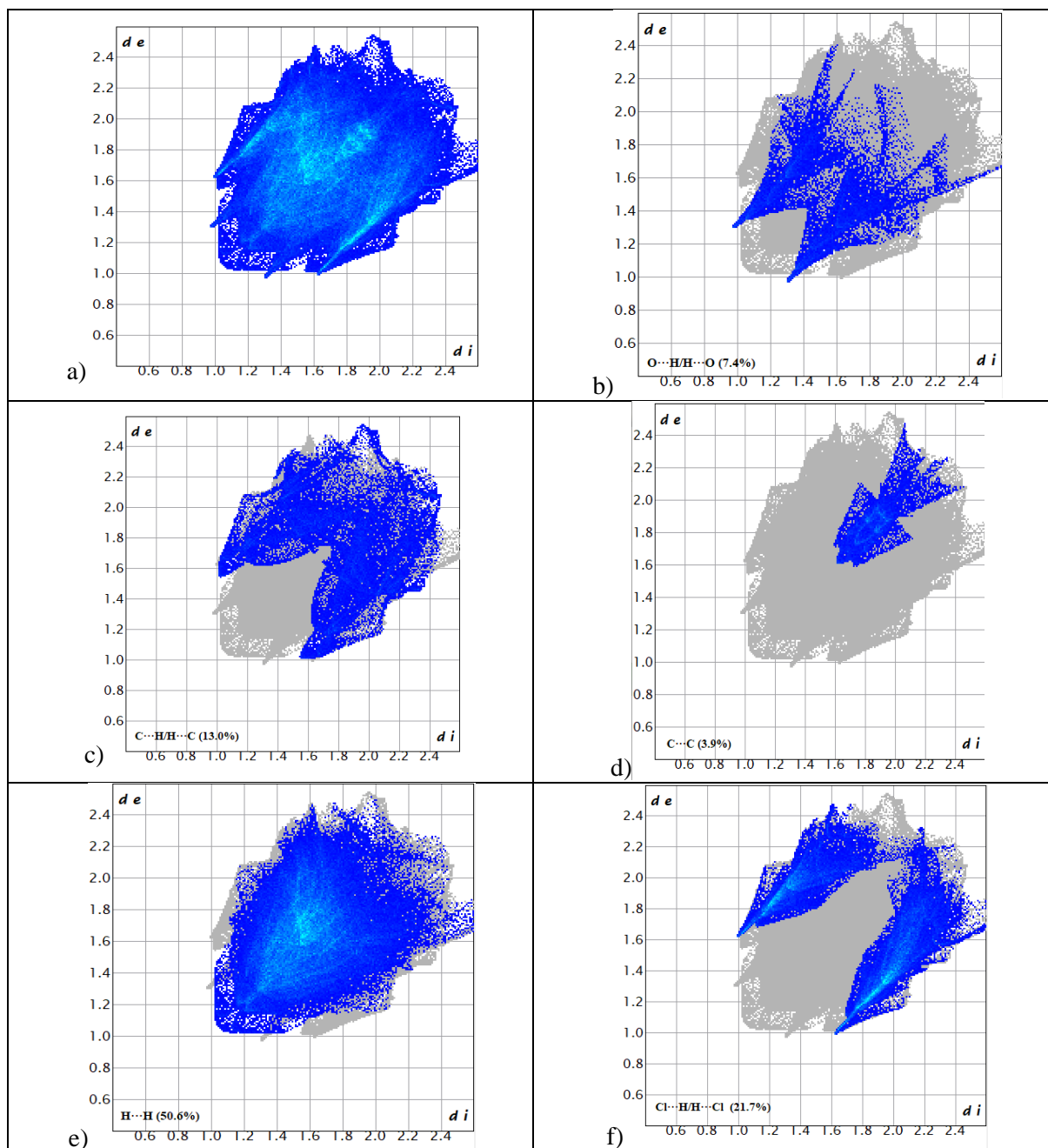


Figure S24 The full two-dimensional fingerprint plots of HAR8 model of prepared complex, showing a) all interactions, b) $\text{O}\cdots\text{H}/\text{H}\cdots\text{O}$, c) $\text{C}\cdots\text{H}/\text{H}\cdots\text{C}$, d) $\text{C}\cdots\text{C}$, e) $\text{H}\cdots\text{H}$, and f) $\text{Cl}\cdots\text{H}/\text{H}\cdots\text{Cl}$ close contacts.

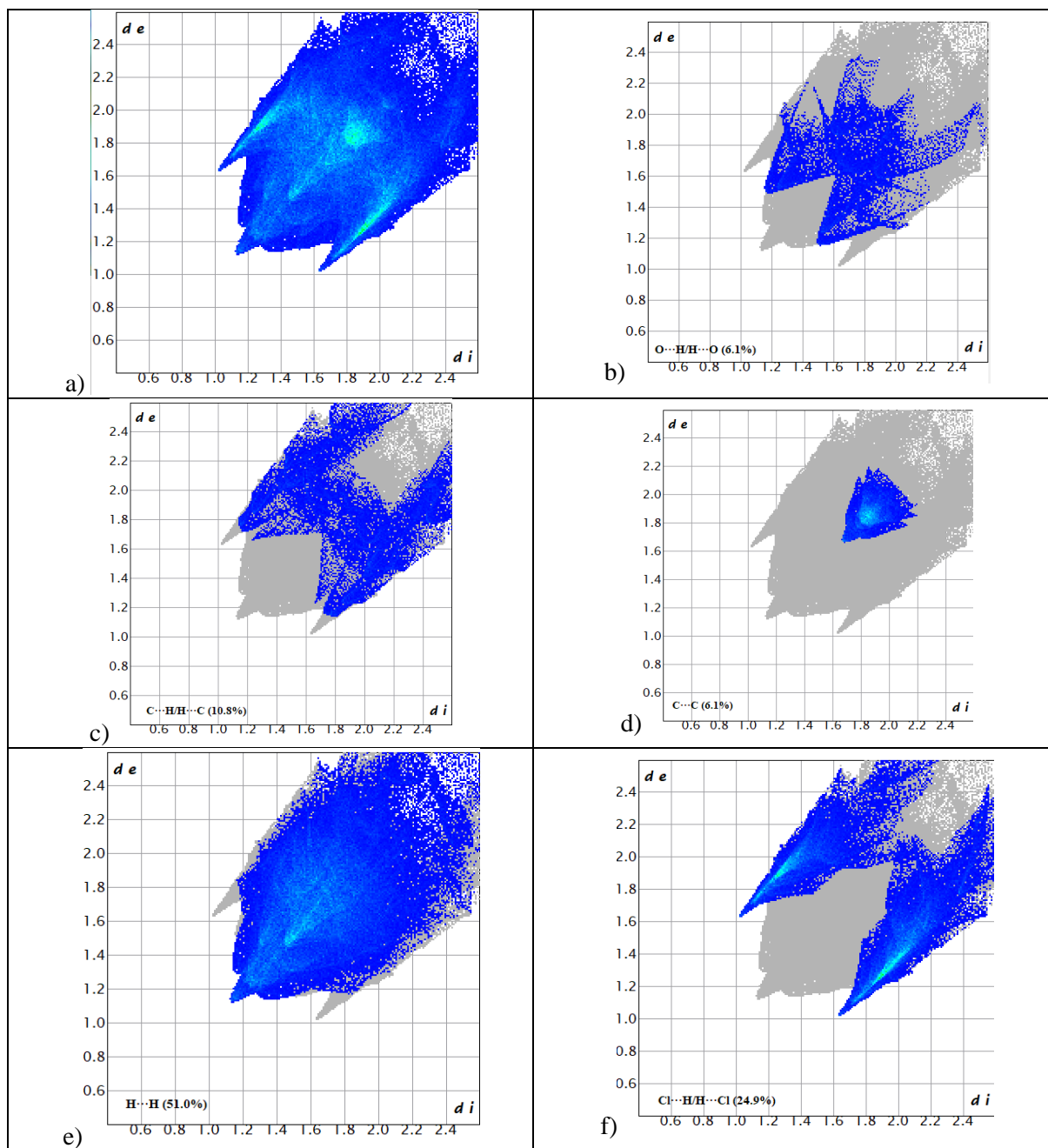


Figure S25 The full two-dimensional fingerprint plots of orthorhombic polymorph [35], showing a) all interactions, b) $O \cdots H/H \cdots O$, c) $C \cdots H/H \cdots C$, d) $C \cdots C$, e) $H \cdots H$, and f) $Cl \cdots H/H \cdots Cl$ close contacts.

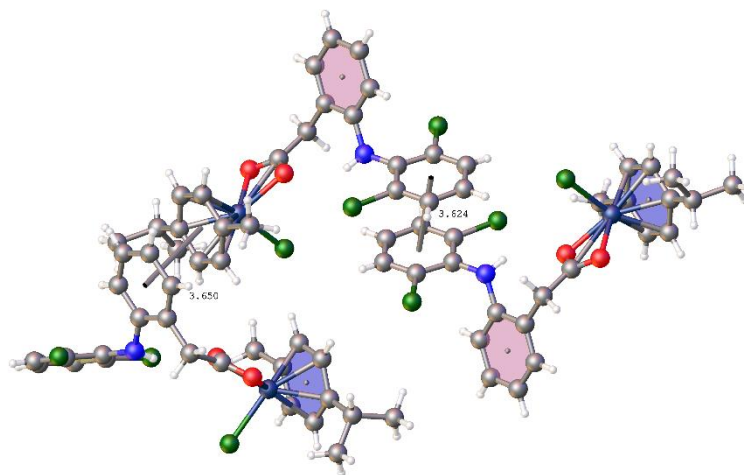


Figure S26 π - π interactions in a polymorph that was previously published [35].

References

35. P. Mandal, B.K. Kundu, K. Vyas, V. Sabu, A. Helen, S.S. Dhankhar, C.M. Nagaraja, D. Bhattacharjee, K.P. Bhabak, S. Mukhopadhyay, Ruthenium(II) Arene NSAID Complexes: Inhibition of Cyclooxygenase and Antiproliferative Activity Against Cancer Cell Lines, Dalton Trans. 2018, 47, 517-527. <https://doi.org/10.1039/C7DT03637J>